

LA-UR--89-2710

DE89 016768

TITLE *Solid Fiber Z-Pinches: "Cold Start" Computations*AUTHOR(S) *Irvin R. Lindemuth, X-1*SUBMITTED TO *Second Int. Conf. on High Density Pinches, Laguna Beach, CA  
April 26-28, 1989***DISCLAIMER**

This report was prepared as an account of work sponsored by an agency of the United States Government. Neither the United States Government nor any agency thereof, nor any of their employees, makes any warranty, express or implied, or assumes any legal liability or responsibility for the accuracy, completeness, or usefulness of any information, apparatus, product, or process disclosed, or represents that its use would not infringe privately owned rights. Reference herein to any specific commercial product, process, or service by trade name, trademark, manufacturer, or otherwise does not necessarily constitute or imply its endorsement, recommendation, or favoring by the United States Government or any agency thereof. The views and opinions of authors expressed herein do not necessarily state or reflect those of the United States Government or any agency thereof.

*Received by mail*

This document contains information which is classified "Secret" under Executive Order 11652, dated 11/18/50, and is to be controlled in accordance with the provisions of that order.

This document is the property of the United States Government and is loaned to your agency; it and its contents are not to be distributed outside your agency.

**Los Alamos** Los Alamos National Laboratory  
Los Alamos, New Mexico 87545

**MAIL ROOM**

MAIL IS UNLIMITED

# SOLID FIBER Z-PINCHES: "COLD-START" COMPUTATIONS

Irvin R. Lindemuth

Los Alamos National Laboratory, Los Alamos, New Mexico 87545

## ABSTRACT

One- and two-dimensional magnetohydrodynamic computations have been performed to study the behavior of solid deuterium fiber Z-pinch experiments performed at Los Alamos and the Naval Research Laboratory. The computations use a tabulated atomic data base and "cold-start" initial conditions. The computations predict that the solid fiber persists longer in existing experiments than previously expected and that the discharge actually consists of a relatively low-density, hot plasma which has been ablated from the fiber. The computations exhibit  $m=0$  behavior in the hot, exterior plasma prior to complete ablation of the solid fiber. The  $m=0$  behavior enhances the fiber ablation rate.

## INTRODUCTION

Experiments at Los Alamos<sup>1</sup>, the Naval Research Laboratory<sup>2</sup>, Imperial College<sup>3</sup>, and elsewhere have demonstrated that interesting fusion plasmas can be created by discharging modern high-voltage pulsed power generators through frozen deuterium fibers or solid fibers of other materials. Experimental diagnostics have led to suggestions that the frozen fiber discharges are stable for 50-100 magnetohydrodynamic instability growth times. Sethian *et al.*<sup>3</sup> have reported that the fiber-formed column remains stable until the driving current reaches a peak, at which time a sudden, rapid expansion and onset of neutron production is observed. Because of the success of existing experiments, new facilities are being built to study the behavior of fiber-formed plasmas at higher current levels.

The author and his colleagues have recently reported<sup>4</sup> one-dimensional magnetohydrodynamic computations which show that current in the existing Los Alamos and Naval Research Laboratory (NRL) experiments is carried by hot plasma which has been ablated from the solid fiber and that the current channel is significantly larger than the initial fiber. The computations have suggested that the presence of a solid fiber core throughout a large fraction of the duration of the existing experiments may play a role in the stability of the plasma column. Although the computed current channel radius agrees with the streak-photograph radius of the NRL experiment, the one-dimensional computations do not provide an explanation of the onset of neutron production.

In this paper, our initial two-dimensional computations of the formation and evolution of the cryogenic fiber pinches are reported. As with our one-dimensional computations, the computations use "cold-start" initial conditions in an attempt to compute the behavior of the pinch from  $t=0$ . The computations model the existing Los Alamos and NRL facilities (250 kA-200 ns and 500 kA

120 ns, respectively) and the new Los Alamos facility under construction (1.2 MA-100 ns).

The computations reported in this paper are a direct extension of our computational capability which was developed to study the laser-initiated z-pinch<sup>5</sup>. As reported in an invited paper<sup>6</sup> presented at the First International Conference on Dense Z-Pinches, our computations of the laser-initiated z-pinch predicted essentially all experimental observations, including the time delay between laser-initiation and the onset of current, the shadowgram diameter, the visible emission, and the temperature determined by x-ray emission.

## MHD MODEL

The magnetohydrodynamic (MHD) model used in our computations includes the continuity equation, an equation of motion, an energy equation, and Faraday's law which is combined with Ohm's law. The equation of motion includes the pressure gradient and Lorentz force but ignores the role of viscosity. The energy equation includes thermal conduction, Ohmic heating, and radiation losses. The model requires for completeness the specific internal energy, the pressure, the thermal conductivity, the average ionization level, the electrical resistivity, and the Planckian opacity as functions of density and temperature. To obtain the equation of state (specific energy and pressure), the ionization level, the resistivity, and the opacity, the computations use the Los Alamos SESAME tabulated atomic data base computer library. The thermal conductivity uses essentially the Braginskii formalism. In the course of a typical computation, all quantities will vary by several orders of magnitude.

## COMPUTATIONAL METHODS

The two-dimensional MHD partial differential equations are solved numerically by an alternating-direction implicit (ADI) finite difference method which is a variant of the Peaceman-Rachford and Douglas-Gunn methods. In principle, the implicit method permits a larger time increment than would be allowed using less sophisticated explicit methods. An important feature of the numerical method used is that all equations are solved simultaneously without resort to fractional time steps, or "operator splitting." In addition to the implicitness and simultaneity of the algorithm, the energy conservation properties of the algorithm depend only upon the time-step size and not the spatial zone size<sup>7</sup>.

The model equations are solved on an  $r$ - $z$  mesh. In the computations reported here, 30 uniformly sized zones in the axial direction are used. Perfectly electrically and thermally insulating boundary conditions are used at the axial boundaries. Two different axial lengths,  $l$ , are considered,  $l=5$  mm and  $l=300$   $\mu$ m, to study long- and short-wavelength behavior. Non-uniform radial zoning is used to adequately resolve both the small initial fiber diameter and the subsequent expansion to large radii. The outer radius of the mesh is 0.6-1 mm and 80-96 radial zones are used.

Instability growth in the computations is monitored by examining the axial kinetic energy. If the pinch column were behaving in a one-dimensional manner, the axial kinetic energy would be zero. On the other hand, in an  $m=0$  instability (the only mode which our two-dimensional model can develop), the axial velocity should increase as  $e^{t/\tau}$  in the linear phase, where  $\tau$  is the growth time, so that the axial kinetic energy should increase as  $e^{2t/\tau}$ .

Even though the outer radius of the computational mesh is much larger than the initial fiber radius, some of the plasma ablated from the solid core eventually interacts with the outer boundary in a way which initiates a non-linear numerical instability, at which time our computations are terminated. The numerical instability seems to occur because large resistive diffusion decouples the equation-of-motion boundary condition<sup>8</sup> from Faraday's law; methods to restore the appropriate coupling are being developed.

## INITIAL CONDITIONS

As in our one-dimensional computations<sup>4</sup>, the "cold-start" initial conditions for the computations reported here are a solid, cryogenic fiber [ $\rho_f = (0.5-1)\rho_s = 88-176 \text{ kg/m}^3$ ;  $T_f = 0.001 \text{ eV}$ ] surrounded by a low density, "warm" halo ( $\rho_h = 0.176 \text{ kg/m}^3$ ,  $T_h = 1-2 \text{ eV}$ ) which has a radius typically 20-30  $\mu\text{m}$  larger than the fiber radius,  $r_f$ . The warm halo is required to provide an initial current conduction path, since the high-density, central fiber is an insulator at low temperature. Parameter studies have shown that our computed results are insensitive to the value of the halo radius except for a short lived ( $<10 \text{ ns}$ ) transient.

To provide perturbations for instability growth, a 2% random perturbation is superimposed upon the density profile of the solid core. No perturbations are superimposed upon the halo. Because the perturbations are random, essentially all wavelengths which the computational mesh can support are present in the initial conditions. Because the number of axial zones is the same in all computations, those with  $l=300 \mu\text{m}$  can support shorter wavelengths than those with  $l=5 \text{ mm}$ .

## COMPUTATIONAL RESULTS

Even though the initial halo is not perturbed, perturbations are present in the low density plasma ablated from the solid core of the pinch because of the perturbations initially in the core. Because the low-density plasma corona is confined by the azimuthal magnetic field, a "classical"  $m=0$  instability initiates rapidly in the hot corona even prior to complete fiber ablation. The  $m=0$  growth is reflected in the axial kinetic energy, which is compared with the thermal energy in Fig. 1 for HDZP-I, the existing Los Alamos facility. The axial kinetic energy exhibits linear growth for over six orders of magnitude. The  $l=300 \mu\text{m}$  case (Fig. 1e) exhibits more rapid growth than the longer case (Fig. 1d). Growth times ( $\tau$ ) are approximately 0.7 ns (Fig. 1e) and 2.2 ns (Fig. 1d). At the time at which the computations were terminated, the growth in axial kinetic energy

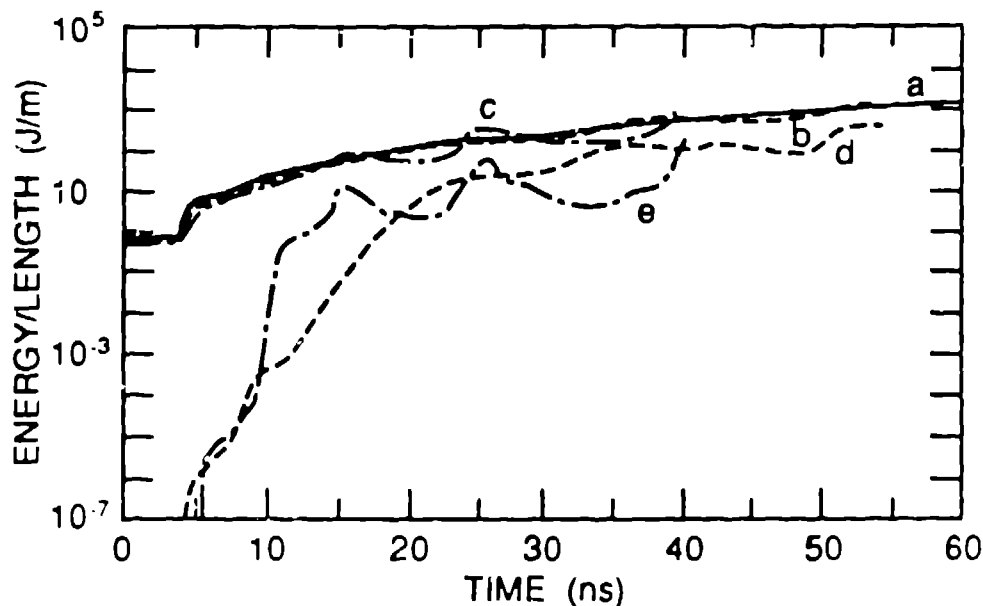


Fig. 1. Thermal energy (a,b,c) and axial kinetic energy (d,e) for a one-dimensional computation (a) and two-dimensional computations with  $l=5$  mm (b,d) and  $l=300$   $\mu$ m (c,e) for HDZP-1 ( $r_f=15$   $\mu$ m,  $\rho_f=0.5$   $\rho_e$ ).

reached a saturation level which was generally an order of magnitude lower than the corresponding thermal energy, and the thermal energy of the plasma column in the two-dimensional cases (Figures 1b,c) does not differ significantly from the one-dimensional case (Fig. 1a).

Even though most of the current flows in the low-density corona, the  $m=0$  behavior which initiates in the corona eventually effects the high-density core. Density contours in the  $r$ - $z$  plane for the two-dimensional computations of Fig. 1 are shown in Figures 2 and 3. In Figures 2 and 3, the contour values are chosen so that 10% of the total pinch mass lies between each set of adjacent contours, with 50% of the mass lying within Figures 2e and 3e. If the pinch behaved in a one-dimensional manner, all contours would be straight and horizontal and reflect the one-dimensional radial density profile (similar to Fig. 1a of Ref. 4). The long-wavelength case (Fig. 2) shows that at 25 ns the solid core is more-or-less intact, even though its radius is somewhat smaller than the 9  $\mu$ m of the corresponding one-dimensional case (Fig. 3c of Ref. 4). On the other hand, even at 20 ns, the short-wavelength case shows essentially no mass at or above the initial density ( $\rho_f=88$  kg/m<sup>3</sup>), and a given mass fraction (e.g., 50%, Figures 2e and 3e) is located at a significantly larger radius than for  $l=5$  mm.

Figures 2 and 3 exhibit qualitatively different behavior. In Fig. 2, the shortest wavelength which the computational mesh can support is evident, whereas in Fig. 3, the shortest wavelengths which the mesh can support are not present and one of the longest wavelengths possible is dominant. Detailed examination

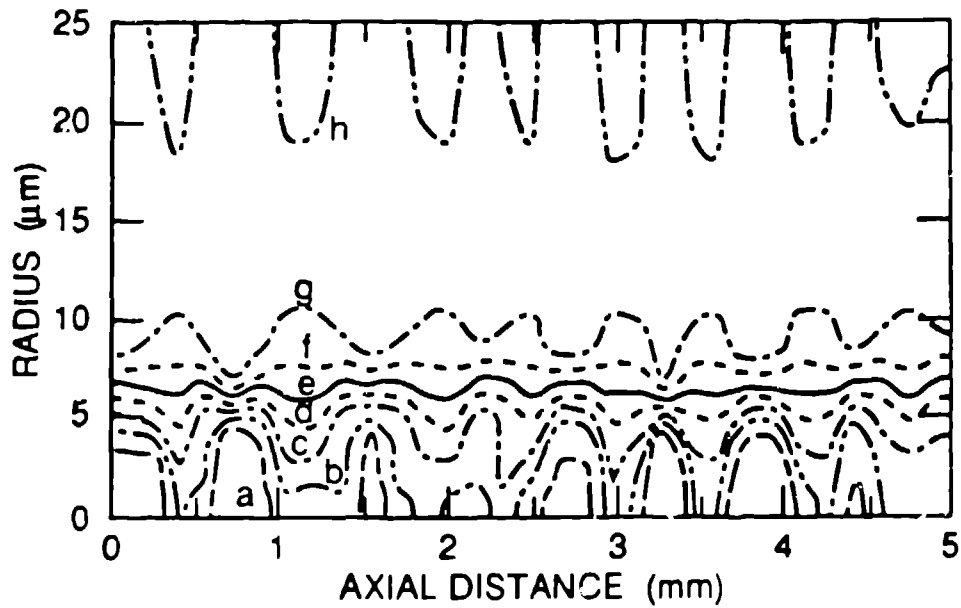


Fig. 2. Mass density contours in the  $r$ - $z$  plane at 25 ns for  $l=5$  mm (HDZP-I,  $r_f=15$   $\mu\text{m}$ ,  $\rho_f=0.5 \rho_s$ ). The contour values are ( $\text{kg}/\text{m}^3$ ): (a) 307; (b) 266; (c) 234; (d) 194; (e) 155; (f) 108; (g) 51; (h) 0.59.

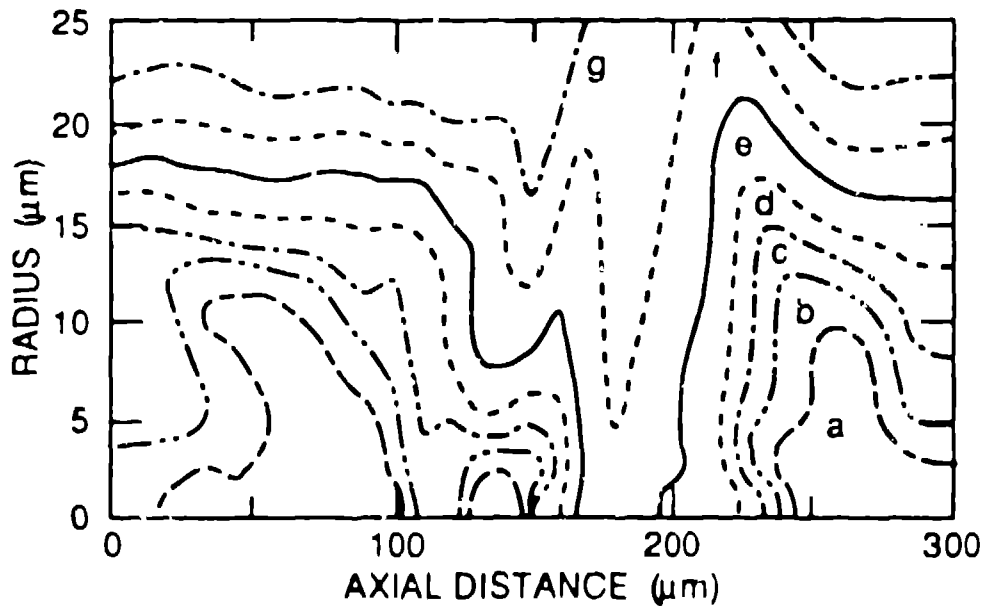


Fig. 3. Mass density contours in the  $r$ - $z$  plane at 20 ns for  $l=300$   $\mu\text{m}$  (HDZP-I,  $r_f=15$   $\mu\text{m}$ ,  $\rho_f=0.5 \rho_s$ ). The contour values are ( $\text{kg}/\text{m}^3$ ): (a) 66; (b) 52; (c) 42; (d) 31; (e) 19; (f) 12; (g) 6.5.

of the  $l=300\text{ }\mu\text{m}$  computations at early time suggest that the shortest wavelengths never grew to a readily detectable amplitude and that intermediate wavelengths rapidly saturated, suggesting a physical mechanism (e.g., resistive diffusion) which rapidly damps wavelengths comparable to the initial fiber radius. Similar behavior for short wavelengths has been observed in computations of the unstable behavior of hot, magnetized plasma in contact with a cold wall<sup>9</sup>. In addition, for times later than 20 ns, the  $l=300\text{ }\mu\text{m}$  computation appears to periodically reestablish a quasi-one-dimensional configuration, followed by subsequent  $m=0$  behavior.

As Figures 2 and 3 indicate, the  $m=0$  behavior enhances the fiber ablation rate and increases the radius of the channel. This effect is illustrated in Fig. 4, which indicates the mass distribution within the channel. Whereas, at 30 ns, the mass distribution for  $l=5\text{ mm}$  (Fig. 4b) is comparable to the one-dimensional case (Fig. 4a), the distribution for  $l=300\text{ }\mu\text{m}$  (Fig. 4c) shows all mass at a considerably lower density and indicates that the fiber has been totally ablated by 30 ns. For  $l=300\text{ }\mu\text{m}$ , the time to complete ablation of the fiber is approximately 21 ns, whereas, for  $l=5\text{ mm}$ , the time for ablation is approximately 55 ns, and, for the corresponding one-dimensional case (Fig. 3c of Ref. 4), approximately 65 ns are required for total fiber ablation.

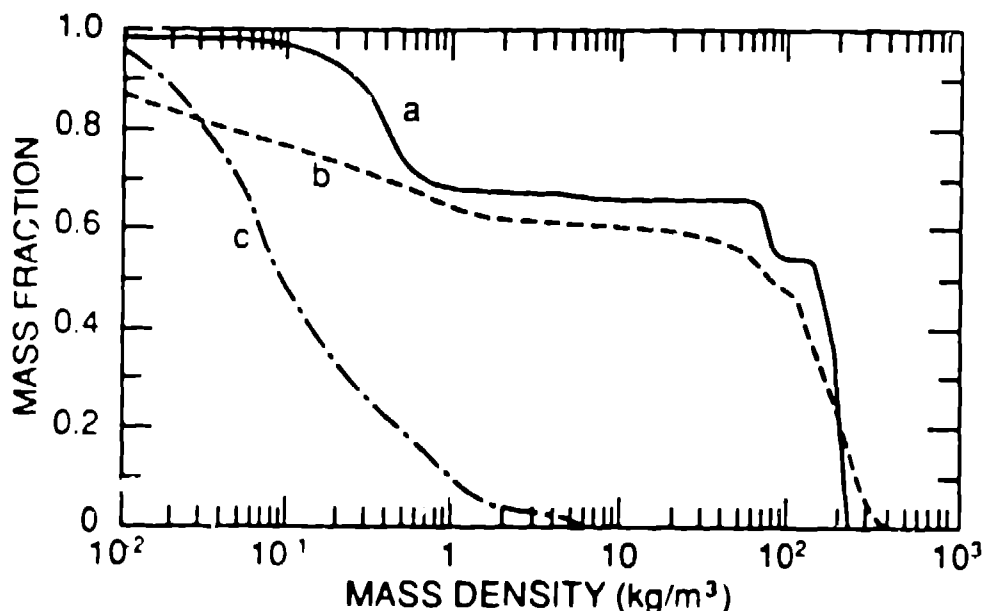


Fig. 4. Mass fraction having a mass density above a value,  $\rho$ , as a function of the mass density,  $\rho$ , at 30 ns (HDZP-I,  $r_f=15\text{ }\mu\text{m}$ ,  $\rho_f=0.5\text{ }\rho_s$ ) for: (a) a one-dimensional computation; (b)  $l=5\text{ mm}$ ; (c)  $l=300\text{ }\mu\text{m}$ .

Our corresponding computations for the existing NRL experiment are qualitatively similar to those for HDZP-I which have been reported above. Even

though the NRL current and  $dI/dt$  is larger than for HDZP-I, the fiber diameter ( $125 \mu\text{m}$ ) is also larger, so that the  $m=0$  growth times and fiber ablation times are correspondingly larger. Computations completed to date indicate growth times of 0.9 ns for  $l=300 \mu\text{m}$  and 2.4 ns for  $l=5 \text{ mm}$ . Whereas one-dimensional computations suggest that the solid core persists throughout the duration of the NRL experiment (Fig. 5a of Ref. 4), two-dimensional  $l=300 \mu\text{m}$  computations show a fiber ablation time of 40 ns, and those for  $l=5 \text{ mm}$ , not yet completed, suggest that the fiber ablation time will be significantly longer than 55 ns.

Our computations for HDZP-II, the Los Alamos facility presently under construction, are also qualitatively similar. However, even one-dimensional computations predict that the fiber will ablate rapidly in approximately 11 ns and not persist for a significant fraction of the duration of the experiment. The fiber ablation time in two-dimensions is essentially the one-dimensional value, 11 ns, for  $l=5 \text{ mm}$  and approximately 6 ns for  $l=300 \mu\text{m}$ , and the corresponding growth times are 1.2 ns and 0.3 ns, respectively. As with HDZP-I (Figures 1a,b,c), the total thermal energy coupled to the plasma is similar in one-dimensional and two-dimensional computations. However, the turbulence which results from the  $m=0$  behavior significantly changes the density and temperature distribution of the plasma channel. The  $m=0$  behavior reduces the average density of the plasma (similar to Fig. 4) and leads to a broader channel which no longer has the uniform temperature distribution of the one-dimensional computations. Shown in Fig. 5 is the temperature distribution for the HDZP-II computations at 15 ns. The 450 eV temperature of over 90% of the mass in the one-dimensional

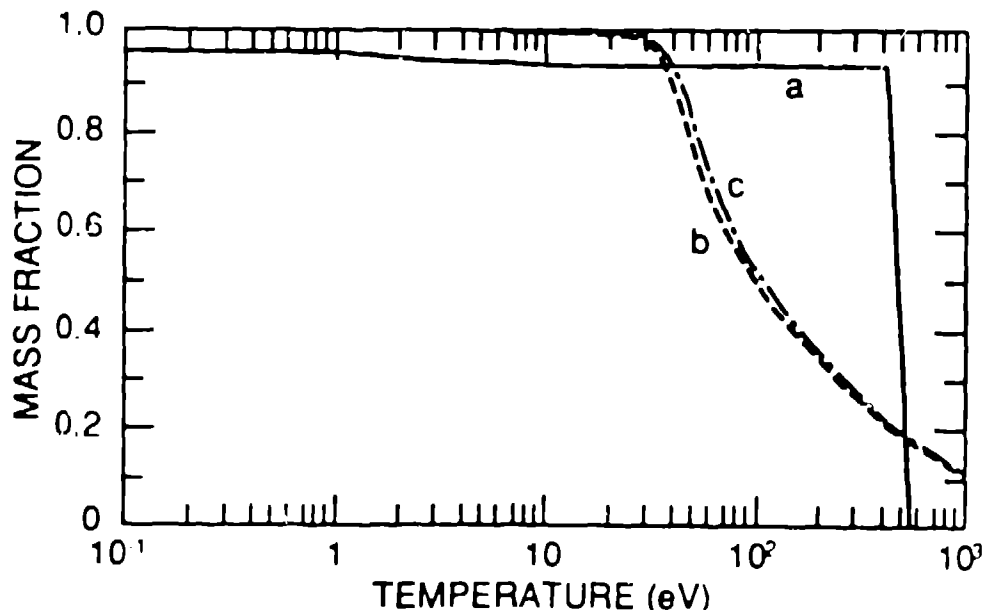


Fig. 5. Mass fraction having a temperature above a value,  $T$ , as a function of the temperature,  $T$ , at 15 ns (HDZP-II,  $r_f=15 \mu\text{m}$ ,  $\rho_f=0.5 \rho_s$ ) for: (a) a one-dimensional computation; (b)  $l=5 \text{ mm}$ ; (c)  $l=300 \mu\text{m}$ .



computation (Fig. 5a) is essentially the Bennett temperature. In contrast, in the two-dimensional computations (Figures 5b and 5c), which are similar, over 80% of the mass is less than the Bennett temperature, although nearly 20% of the mass is at a significantly higher temperature.

Under some circumstances not yet understood, hot spots form in the computations at the boundary of the solid core as a result of the  $m=0$  behavior in the corona. Furthermore, the hot spots have been observed to move axially as the "bubbles" of the  $m=0$  instability move radially inward. The existence of such hot spots has been observed experimentally by the Imperial College group using an optical fiber rather than frozen deuterium. The Imperial College group reported<sup>3</sup> that

"Time integrated soft X-ray pinhole photographs show a plasma column with a radius four times larger than the initial fiber...The variation of the intensity along the column has a scale length which is consistent with the characteristics of the instabilities observed with the optical diagnostics. Most strikingly, the intensity is peaked at the surface of the column. This clearly indicates that the plasma is formed on the surface of the fiber and that at the time of maximum X-ray emission there exists a sizeable core of the fiber that is not ionized."

## CONCLUDING REMARKS

In contrast to the interpretations of the experimental data, our initial two-dimensional computations suggest that fiber-formed z-pinches are, in fact, unstable. There is an apparent contradiction, the resolution of which is beyond the scope of this paper, although some discussion is appropriate. If, in fact, the experiments are stable, then the computations are in error, suggesting that physical mechanisms not included in the computations (e.g., viscosity) are playing a stabilizing effect. Various authors, including several in these Proceedings, are exploring various possible stabilizing mechanisms.

On the other hand, it is not obvious that the computations reported here are inconsistent with the experimental observations. It is presently believed<sup>10</sup> that the solid fiber in the HDZP-I experiment has been totally ablated somewhat earlier than in our one-dimensional computations<sup>4</sup>, perhaps suggesting the two-dimensional behavior reported here. Certainly, the computed persistence and behavior of the solid fiber core are qualitatively consistent with the Imperial College observations (although it is quite plausible that the optical fiber used by Imperial College may behave differently than the frozen deuterium of Los Alamos and NRL). In addition, the fact that the computed one-dimensional channel radius for the NRL experiment is somewhat less than the observed streak-photograph radius (Fig. 5 of Ref. 4) may also be indicative of the

two-dimensional behavior reported here. An important step which we have yet to make is to actually compute the optical diagnostics (streak photograph, Schlieren photograph, etc) which would result if a plasma having the density and temperature profiles of our two-dimensional computations was actually present in an experiment. The periodic reestablishment of a quasi-one-dimensional configuration in the short wavelength computations raises the possibility that the plasma may be so  $m=0$  turbulent that it appears to be homogenous in the diagnostics which have been implemented to date.

The two-dimensional computations completed to date, to the extent that they have been analyzed, do not appear to either confirm or refute our previous speculation<sup>4</sup> that, in existing experiments, the fiber ablation process may play an important role in the behavior of the pinch and that neutron production may occur at the time of complete fiber ablation. There does not appear to be any major qualitative change in behavior in the computations when the fiber has ablated. Our computations clearly suggest the need for advanced diagnostic techniques to definitively detect the presence or absence of a high-density, cold core.

Our computations predict that the fiber will become ablated very rapidly in HDZP-II, the Los Alamos facility under construction. Hence, any stabilizing property of the fiber ablation process is not likely to play an important role. Our computations would suggest that, even in the presence of  $m=0$  behavior, very interesting fusion plasmas may still persist for a significant amount of time. Although the  $m=0$  behavior appears computationally to enhance the plasma expansion rate, there is as yet no indication that the behavior is totally disruptive during the anticipated duration of the experiment. The enhanced expansion, as suggested by Fig. 4 and predicted by Fig. 5, may reduce the neutron yield below that predicted by one-dimensional simulations, but, on the other hand, the hot spots which result from  $m=0$  behavior may actually enhance the neutron yield. The computations appear to provide an indication that, at the high densities characteristic of the fiber-formed pinches, unstable behavior is not necessarily fatal in a fusion context.

Future extensions of the work reported here would include extending the computations to longer times, investigating the behavior of other wavelengths, and studying, in two-dimensions, the behavior of a z-pinch plasma as the Pease-Braginskii current is approached and exceeded.

## ACKNOWLEDGEMENTS

The author would like to acknowledge stimulating discussions on experimental details, computational techniques, and theoretical models with J. Chittenden, A. Glasser, M. Haines, J. Hammel, R. Lovberg, G. McCall, D. Mosher, R. Nebel, A. Robson, P. Sheehey, D. Scudder, J. Sethian, J. Shlachter, and S. Stephanakis.

This work was performed under the auspices of the U. S. Department of Energy. Los Alamos National Laboratory is operated by the University of California for the United States Department of Energy under Contract No. W-7405-ENG-36.

## REFERENCES

- <sup>1</sup>D. W. Scudder, *Bull. Am. Phys. Soc.* **30**, 1408 (1985); also, see Los Alamos papers in these Proceedings.
- <sup>2</sup>J. D. Sethian, A. E. Robson, K. A. Gerber, and A. W. DiSilva, *Phys. Rev. Lett.* **59**, 892 (1987); also, see Naval Research Laboratory papers in these Proceedings.
- <sup>3</sup>M. G. Haines, J. Bailey, P. Baldock, A. R. Bell, J. P. Chittenden, P. Choi, M. Coppins, I. D. Culverwell, A. E. Dangor, E. S. Figuera, and G. J. Rickard, in *Proceedings of the 12th International Conference on Controlled Fusion and Plasma Physics* (Nice, France, 1988).
- <sup>4</sup>I. R. Lindemuth, G. H. McCall, and R. A. Nebel, *Phys. Rev. Lett.* **62**, 264 (1989).
- <sup>5</sup>I. R. Lindemuth, J. H. Brownell, T. A. Oliphant, and D. L. Weiss, *J. Appl. Phys.* **53**, 1415 (1982).
- <sup>6</sup>I. R. Lindemuth, in *Proceedings of the First International Conference on Dense Z-Pinches for Fusion*, edited by J. Sethian and K. Gerber (Naval Research Laboratory, Washington, D.C., 1984), p. 46.
- <sup>7</sup>I. R. Lindemuth, *J. Comp. Phys.* **18**, 119 (1975); errata, *J. Comp. Phys.* **19**, 338 (1975).
- <sup>8</sup>I. R. Lindemuth, *J. Comp. Phys.* **25**, 104 (1977).
- <sup>9</sup>I. R. Lindemuth, J. S. Pettibone, J. C. Stevens, R. C. Harding, D. M. Kraybill, and L. J. Suter, *Phys. Fluids* **21**, 1723 (1978).
- <sup>10</sup>J. E. Hammel, private communication.